Tatiana Cuervo Blanco[1], César A. Sierra[2], Hugo R. Zea[1,*]

[1]Grupo de Investigación en Materiales, Catálisis y Medio Ambiente, Departamento de Ingeniería Química y Ambiental, Universidad Nacional de Colombia, Bogotá, Colombia
[2]Grupo de Investigación en Macromoléculas, Departamento de Química, Universidad Nacional de Colombia, Bogotá, Colombia.

***Autor para correspondencia:** hrzear@unal.edu.co

Recibido: 29 de Abril de 2016. Aceptado: 15 de Junio de 2016.

Nanostructured MnO_2 catalyst in *E. crassipes* (water hyacinth) for indigo carmine degradation

Abstract

The use of water hyacinth's dried matter (*Eichhornia crasippes*) as a support matrix for nano-MnO_2 and its application for the removal of indigo carmine (IC) was studied. Different pretreatment processes were tested and results indicated that an acid-alkali pretreatment is an efficient method to binding nanoparticles (NPs) to cellulosic matrix. In adittion, the MnO_2 NPs were synthesized by sonochemical reduction of MnO_4^- using different methods (ultrasonic horn system, ultrasonic bath and reaction with ethanol), where the influence of the precursor concentration was observed. The synthesized material was further characterized by ATR-IR, AAS, XRD, SEM, nitrogen isotherms adsorption, EDS, and pH_{pzc}. The IC removal capacity of the nanostructured material, the chemical nature of the degradation products and the effect of various parameters (temperature, pH, initial IC concentration, among others) were explored in water samples.

Keywords: *Eichhornia crassipes*, indigo carmine, nanostructured material, manganese oxide.

Catalizador de MnO_2 nanoestructurado en *E. crassipes* (jacinto de agua) para la degradación de índigo carmín

Resumen

Se estudió el uso de la materia seca del jacinto de agua (*Eichhornia crassipes*) como matriz-soporte para nano-MnO_2 y su eficiencia en la eliminación de índigo carmín (IC). Se ensayaron diferentes procesos de pretratamiento y los resultados indicaron que un tratamiento previo ácido-alcalino es un método eficiente para unir las nanopartículas (NPs) a la matriz celulósica. Así mismo, las NPs de MnO_2 se sintetizaron por reducción sonoquímica de MnO_4^- utilizando diferentes métodos (un sistema emisor de ultrasonido, baño de ultrasonido y reacción convencional con etanol como medio). El material sintetizado se caracterizó por ATR-IR, AAS, DRX, SEM, isotermas de adsorción de nitrógeno, EDS y pH_{pzc}. Se exploró la capacidad de eliminación de IC por parte del material nanoestructurado y la naturaleza química de los productos de degradación en muestras acuosas. Se analizó el efecto de diversos parámetros tales como temperatura, pH, concentración inicial de IC, entre otros.

Palabras clave: *Eichhornia crassipes*, índigo carmín, materiales nanoestructurados, óxido de manganeso**.**

Catalisador de MnO_2 nanoestruturado em *E. crassipes* (jacinto da água) para a degradação do índigo carmim

Resumo

Foi estudada a utilização de matéria seca de jacinto de água (*Eichhornia crassipes*) como matriz de suporte para nano-MnO_2 e sua aplicação para a remoção de índigo carmine (IC). Diferentes processos de pré-tratamento foram testados e os resultados indicaram que o prétratamento ácido-álcali é um método eficiente para ligar os NPs à matriz celulósica. Além disso, as NPs de MnO_2 foram sintetizados por redução sonoquímica de MnO_4^- utilizando diferentes métodos (um sistema emissor de ultrassom, banho de ultrassom e a reacção com o etanol). O material sintetizado foi caracterizado por ATR-IR, AAS, DRX, SEM, isotermas de adsorção de nitrogênio, EDS e pH_{pzc}. A facilidade de remoção de IC por o material nanoestruturado e a natureza química da degradação dos produtos foram explorados em amostras aquosas, assim mesmo foi estudado o efeito de vários parâmetros (temperatura, pH, concentração inicial de IC e a quantidade de nanocompósito, entre outros).

Palavras-Chave: *Eichhornia crassipes*, índigo carmim, material nanoestruturado, óxido de manganês.

Rev. Colomb. Quim. **2016**, *45* (2), 30-38. DOI: http://dx.doi.org/10.15446/rev.colomb.quim.v45n2.60395

Introduction

Nowadays, large amount of several synthetic dyes are used in textile, pharmaceutical, cosmetics, beverages, and electronic components industries. Around 10-15% of these dyes, employed by textile industry, are released into effluents, polluting both surface and ground water (*1, 2*).

Indigo (IN) or 2,2'-bis-indole, a blue synthetic dye, is one of the most consumed dyes in the industry, mainly employed for clothes dyeing. In order to enhance its solubility and improve the dyeing process, IN is often transformed into indigo carmine (IC) (indigo disulphonic 5-5') (*3, 4*). However, in spite of its extensive use, IC has been linked to high toxicity (*5*).

The environmental and health concern of these potential pollutants in water has drawn attention of many researches (*6*). In this regard, the application of metal oxide nanoparticles for treatment of contaminated effluents by dyes has become another challenging field in recent years. Manganese oxides, for instance, exhibit outstanding structural multiformity as well as special magnetic and electrochemical properties. Therefore, manganese oxide catalysts show considerable activity in oxidation-reduction reactions (*7-9*).

Similarly, nanomaterials have wide applications as catalysts for dyes degradation (*1*, *7-11*). The application of metal oxides in nano-size, however, has several engineering limitations that restrict its large-scale implementation. For example, these materials occasionally cause the leaching of nanoparticles (NPs), along with the treated effluent, resulting in even more serious environmental problems. Some of these limitations can be prevented by anchoring the nanoparticles on suitable matrices (*9*).

The water hyacinth (WH, *Eichhornia crassipes*), which is a widely prevalent aquatic weed in India, Australia, Africa, and South America, reproduces itself in five days under favorable conditions, obstructs oxygen transfer in water bodies and affects aquatic ecosystems. For this reason, it is considered one of worst invasive aquatic plants (*12, 13*). In spite of that, WH is an inexpensive, readily available biomass resource, which has been widely investigated for its high adsorption capacity (*2*, *14-16*).

For the previous reasons, in this research, the use of dried matter of WH as a support matrix for MnO_2 NPs for removing IC from waste effluents was studied.

Materials and methods

Materials

Fresh WH plants were raised from stolons obtained from Muña Dam area in Colombia. The plants were placed in a clean water reservoir (4° 35'10''N, 74°18′ 0″W) at environmental conditions (day/night temperatures: 13-11°C/10-8°C). After the plant has reached an approximate length of 35 cm, the plants were extracted, washed several times, and dried at 80 ºC for 24 h. Then, they were cut into small pieces (5 to 3 cm in length), and finally the plants were grounded with a ball mill.

Reagents

Potassium permanganate, sodium hydroxide, sulfuric and hydrochloric acid, indigo carmine, and ethanol, were purchased from Sigma Aldrich®. All chemicals and reagents used were analytical grade and used as received.

WH pretreatment

The biomass samples were treated at different pretreatment conditions. In all cases, the biomass was dried at 80 °C for 24 h after each pretreatment (Diagram 1).

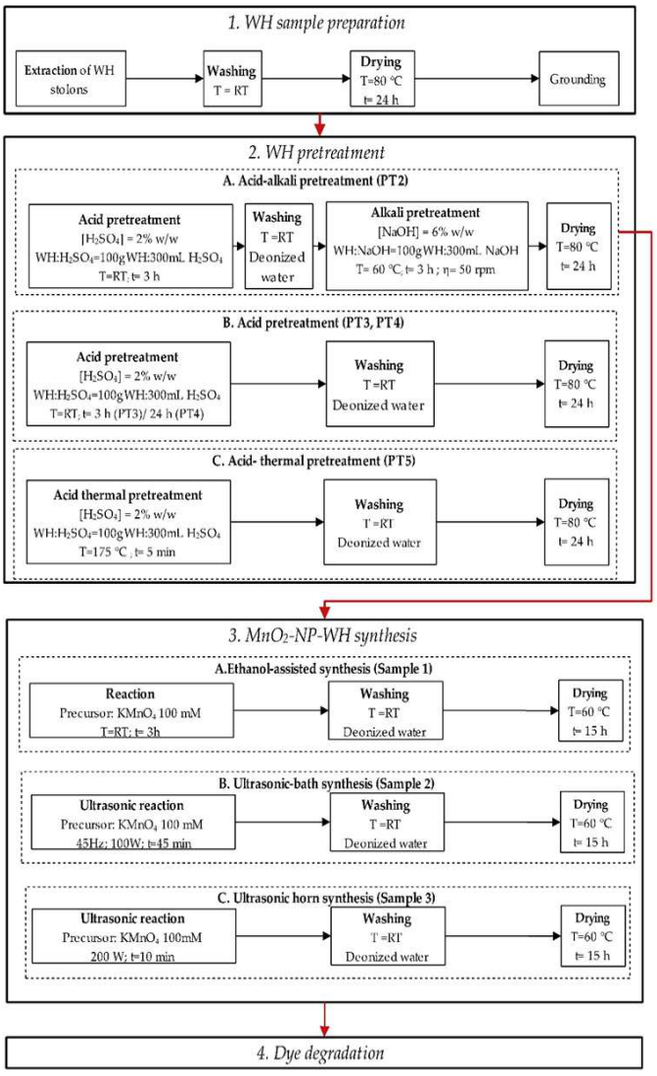

Diagram 1. Description of methodology

Acid-alkali pretreatment (PT2)
Prepared biomass was immersed in a 2% (*v/v*) H_2SO_4 aqueous solution for 3 h at room temperature. After that, it was immersed in a 6% (w/v) NaOH aqueous solution for 3 h at 60 °C.

Acid pretreatments (PT3 and PT4)
Prepared biomass was immersed in a 2% H_2SO_4 (*v/v*) aqueous solution for 3 h (PT3) and 24 h (PT4) at room temperature.

Acid-thermal pretreatment (PT5)
Prepared biomass was immersed in a 2% H_2SO_4 (*v/v*) aqueous solution for 5 min at 175 °C.

MnO_2-NP-WH synthesis

The bionanocomposite obtained by PT2 was synthesized by three different methods (Diagram 1).

Ethanol-assisted synthesis (sample 1)
After analysis of pretreatment methods, PT2 sample was immersed in a $KMnO_4$ (100 mM) solution for 3 h. Ethanol was added drop-wise under constant stirring conditions leading to the formation of a brownish precipitate of MnO_2.

Ultrasonic-bath synthesis (sample 2)
Pretreated biomass was immersed in the precursor solution $KMnO_4$ (100 mM) and the mixture was irradiated with ultrasound waves (45 Hz, 100 W) in a Branson 2510DTH (Bransonic® Sigma-Aldrich) for 45 min.

Ultrasonic horn synthesis (sample 3)
Pretreated biomass was submerged in the precursor solution $KMnO_4$ (100 mM) and the mixture was irradiated with ultrasound waves using an ultrasonic horn of a Sonifier® S-250D operating at 200 W for 10 min. The formation of MnO_2 was verified by UV-Vis at 530 and 320 nm for MnO_4^- and MnO_2, respectively.

Dye degradation experiments and catalyst reuse

The degradation tests were performed in 50 mL of IC solution (concentration range of 20-800 ppm) at 150 rpm, at several pH (2.3, 4.5 and 7.0) and changing the temperature (23, 40 and 60 ºC). A known amount of MnO_2-NP-WH (500 mg) catalyst was added to this solution and the degradation process was followed using the corresponding absorbance at λ = 600 nm (UV-Vis spectra were measured in a Thermo Scientific Evolution 300 UV-Vis spectrophotometer). Control experiments were done with non-modified WH, pretreated WH, and also activated carbon, evaluated as absorbent solid. Before the degradation reaction took place, the pH of the IC initial solution was adjusted by adding 0.2M HCl or 0.1 M NaOH to the reaction mixture in order to evaluate different pH conditions.

Finally, the reuse potential of MnO_2-NP-WH catalyst was tested without previous regeneration, that is, after attaining equilibrium (according to UV-Vis), the used MnO_2-NPWH was carefully removed from the just degraded solution and immediately immersed in a new IC solution, which was monitored again by UV-Vis. To verify the IC degradation capacity, several cycles of consecutive adsorption studies were performed.

Characterization

The moisture content of WH samples was determined using an AMB 50 Moisture Balance Adam Equipment. In addition, ATR-IR spectra were taken with a Nicolet™ iS™ 10 FT-IR Spectrometer (Thermo Fischer Scientific) at 4000-650 cm^{-1}. The surface area of the samples was measured using an AUTOSORB®-1 Series (Quantachrome Instruments); XRD analysis was performed on a PANalytical X'Pert PRO MRD diffractometer; SEM analysis was taken on a LEO 1550 SEM/EDS instrument. Before EDX analysis, the samples were coated with 3 nm platinum and the micrographs were taken at 10 kV. Moreover, a Thermo Electron S4 AA spectrometer, equipped with a manganese hollow cathode lamp and an acetylene-air flame, was used for the atomic absorption spectroscopy analyses (AAS) to quantify the Mn content, deposited on the WH (following the National Environment Protection Council procedure (*17*)), and to determine de Mn, leached to the reaction mixture (*17*).

IC degradation products were identified by mass spectrometry (MS) using a Bruker Daltonics amaZon X, ESI-Ion Trap Mass Spectrometer operating in negative mode. pH at the point of zero charge (pH_{pcz}) was determinate using titration methodology; 45 mL of KNO_3 to 1% (*v/v*) were adjusted for initial pH in the range of 2 to 10 by adding HCl 0.1 M or NaOH 0.1 M, the volume of each solution was completed up to 50 mL by adding KNO_3 to 1% (*v/v*); 0.1 g of fique fiber (raw, pretreated or cationizated) was added and kept under constant temperature (25 °C) and agitation for 24 h and then pH values of the supernatants were registered.

Results and discussion

Dye degradation experiments and catalyst reuse

The objective of the biomass pretreatment was the removal of lignin and hemicellulose, cellulose crystallinity decrease, and the material porosity improvement, so that MnO_2 NPs could effectively bind to the cellulose matrix. According to Table 1, the acid-alkali pretreated WH (PT2) exhibited the largest surface area (6.74 m^2/g), which is six times the surface area showed by the WH biomass before any chemical modification. Although the surface area of WH biomass reported by others (1.80-4.50 m^2/g) (*14-16*) clearly differs from the value found in this study (1.28 m^2/g), this could be explained by the different growth conditions of the WH plants evaluated in each study.

Table 1. Surface area for pretreated WH

Sample	Surface area (m^2/g)
WH	1.28
Pretreated WH (PT2)	6.74
Pretreated WH (PT3)	3.56
Pretreated WH (PT4)	5.44
Pretreated WH (PT5)	6.57
Comercial Activated Carbon	634.2

Lignin, hemicellulose, and cellulose content onto the WH biomass surface after the pretreatment, was evaluated by ATR-IR, and the results suggested, similarly to previous reported studies in other lignocellulosic materials (*18-20*), that the combined pretreatment method acid-alkali (PT2) is the best suitable method to obtain much better activated biomass surface (Figure 1). The normalized FT-IRs show that the acid-alkali pretreatment increases the –OH signal in comparison with the WH untreated, which suggest that more –OH groups are exposed, leading to a higher number of centers for NPs growth. This is further supported by the increase of the signals for C-O-C bonds (1008-1109 cm-1), assigned in previous reports to an increase in the cellulose content on the material surface. In other words, PT2 has a lower lignin-hemicellulose and greater cellulose content than any other sample analyzed, including the WH untreated.

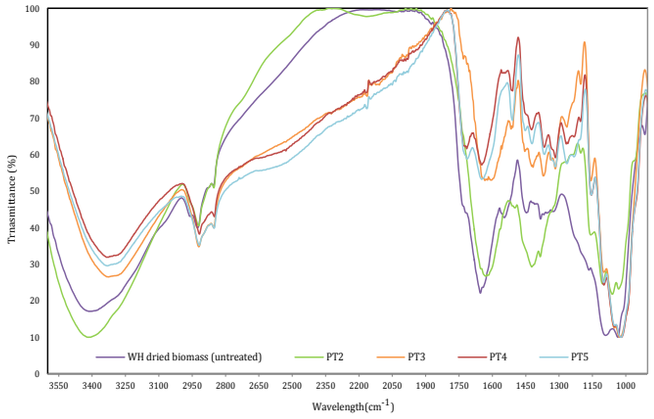

Figure 1. AT-IR spectra of the pretreated WH samples

The positive results for the combined acid-alkali pretreatment can be explained because the H_2SO_4 pretreatment can effectively dissolve the hemicelluloses (xylan) and increase the enzymatic digestibility of cellulose, achieving high reaction rates in comparison with the enzymatic processes (*21, 22*). Furthermore, it is known that the main effects of NaOH pretreatment on lignocellulosic materials, such as the WH biomass are, firstly, the delignification by breaking the ester bonds cross-linking lignin and xylan, and secondly, the increase of the hemicellulose solubility (*19, 23*).

Due to this alkali pretreatment, a large number of hydroxyl groups (R-CH_2-OH), contained in the biological tissues, are converted in salts (R-CH_2-ONa) and incorporated into the biological templates. Because of the resulting high porosity and ionic environment, the MnO_4 accesses the hierarchical pore channels and forms MnO_2 NPs inside the pores more easily (*19*). Additionally, the NaOH causes the swelling of the biomass, which increases the internal surface area of the WH and decreases the cellulose crystallinity (*24*).

NP synthesis

As mentioned above, for this study the NPs deposition was carried out by two principal methods: ethanol and ultrasonic assisted synthesis (sonochemical reaction). In both cases, the pretreated yellowish WH biomass (obtained after PT2) was immersed in the $KMnO_4$ precursor solution to replace Na^+ for MnO_4^- ions into the R-CH_2-ONa centers formed during the pretreatment. Subsequently, the MnO_4^- ions over the WH surface were reduced either by the addition of ethanol or by the ultrasonic waves to finally deposit MnO_2 NPs onto the WH.

On the one hand, in the ethanol-assisted synthesis, the $KMnO_4$ present in the precursor solution acts as an oxidizing agent in neutral medium, water in this case. The ethanol is oxidized into acetic acid and permanganate is reduced, leading to the precipitation of MnO_2 and to the KOH formation (*25*). On the other hand, and regardless the ultrasonic waves generation method (bath or horn), the sonochemical reduction of MnO_4^- proceeds according to the following reaction [1], where the H_2 comes from the sonochemical dissociation (by radicals formation) in the aqueous solution.

$$2MnO_4^-{}_{(aq)} + 3H_{2(g)} \rightarrow 2OH^-{}_{(aq)} + 2H_2O_{(l)} \quad [1]$$

In other words, acoustic cavitation from ultrasonic synthesis produces reactive radicals, which exhibit extremely high cooling rates and can effectively reduce metal ions to metallic nanoparticles or metal oxide nanoparticles (*19, 20*).

In this study, the formation of MnO_2 was verified by UV-Vis at 530 and 320 nm for MnO_4^- and MnO_2, respectively; and the pH values during the synthesis were verified too. In this regard, the pH increases from 7.3 to around 11.2 during the reactions, due to the production of OH^- ions ([1]). An abrupt change of color was observed after all synthetic methods, starting from the characteristic dark purple of aqueous permanganate to a yellowish color at the end of the reaction, similar to the observations reported in other studies (*20*).

Characterization

As mentioned above, the AAS technic was used to quantify the Mn content deposited on WH, following the National Environment Protection Council procedure (*17*). The highest percentage of Mn on WH surface was found for sample 1 (33.3%, *w/w*), which could be explained by the longest contact time of the activated WH biomass with the $KMnO_4$ solution (100 mM, 3h). On the contrary, the ultrasonic syntheses (sample 2 and 3) were performed during 45 and 10 min and the percentages of Mn deposited on each of these surfaces were 21.7 and 28.8% (*w/w*), respectively (Table 2). The periods of time for each method were determined according to the equipment capacity and previous studies reporting successful MnO_2 NPs synthesis at the same conditions. According to the analysis by electron microscopy, the Mn particles deposited on the WH biomass have at least one dimension in the order of nanometers, it is possible to say that most of Mn was deposited as NPs.

Table 2. Mn content on WH by different NPs synthesis methods

Sample	**MnO_2**-NP-WH synthesis	Contact time (min)	Mn on WH (%, *w/w*)
MnO_2-NP-WH (Sample 1)	Ethanol assisted	180	33.32
MnO_2-NP-WH (Sample 2)	Ultrasonic-bath	45	28.74
MnO_2-NP-WH (Sample 3)	Ultrasonic horn	10	21.67

Although the percentages of Mn deposited on samples 2 and 3 were both lower in comparison with sample 1, the contact time for the NPs synthesis related with each method must be taken into consideration: sample 1 needed more than 4 times the contact time needed by sample 3 and approximately 21 times the contact time needed by sample 2, suggesting that the ultrasonic synthesis is more effective for the case of study.

The synthetized MnO_2-NP-WH catalyst, as well as the untreated and the acid-alkali pretreated WH (PT2), were analyzed by XRD in order to describe the crystallinity and structural properties before and after the MnO_2 NPs formation. The XRD patterns showed in all cases a peak around 2θ=23° (Figure 2a), which has been attributed to the high intensity (002) plane of crystalline cellulose (*9, 26*). At this 2θ, WH PT2 showed the most intense peak, confirming that the cellulose content increases as a consequence of the pretreatment, in comparison to the dried WH.

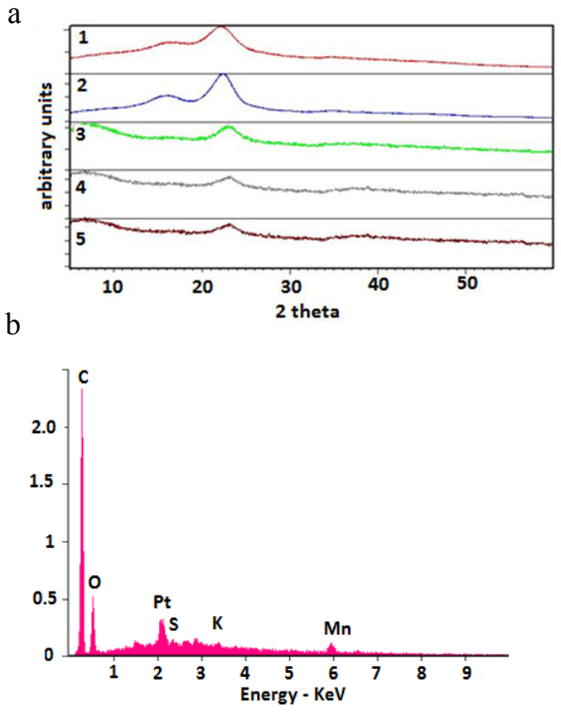

Figure 2. a) XRD spectra for: 1. WH dried grounded biomass; 2. PT2; 3. MnO_2-NP-WH sample 1; 4. MnO_2-NP-WH sample 3; 5. MnO_2-NP-WH sample 2. **b)** EDS analysis of MnO_2-NP-WH sample 1 surface

Moreover, the XRD patterns showed no further visible changes and no peak corresponding to MnO_2, even for the bionanocomposites MnO_2-NP-WH synthesized under different conditions. This might be attributed to the presence of very small crystals, which are apparently below the detection limit of XRD or might be due to the amorphous nature of the MnO_2 prepared (*9*). The EDX analysis of bionanocomposite MnO_2-NP-WH-sample 1 (Figure 2b) showed the characteristic signal for Mn at 5.92 eV. These XRD and EDX results coincide with previously reported studies of MnO_2 NPs synthesized under similar experimental conditions (*1, 20, 27*). The EDX spectrum also showed a signal of Pt around 2.10 eV, which corresponds to the Pt coating used for the analysis.

The scanning electron micrographs of MnO_2-NP-WH-sample 1 exhibited a surface texture, porosity, and cavities of high irregularity (Figure 3a) with elongated hollows of 1-3 µm (Figure 3b), in which the deposition of spherical agglomerated MnO_2 NPs occurred (Figure 3c). All these in agreement with previous reports of MnO_2 NPs (*26*).

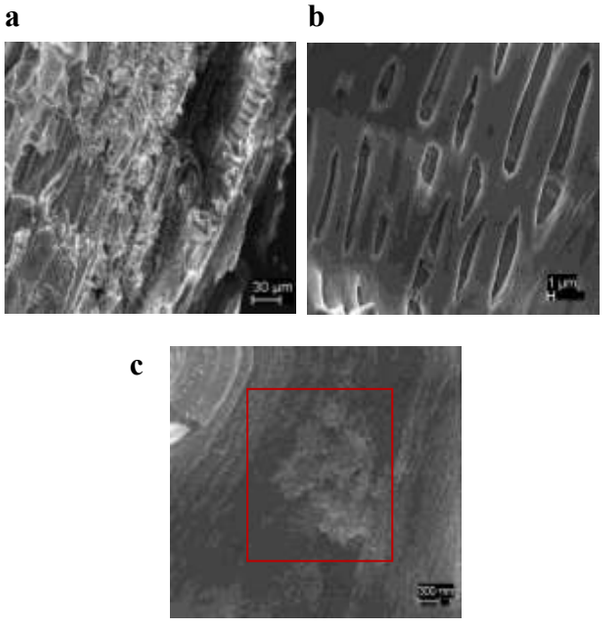

Figure 3. SEM images of MnO_2-NP-WH sample 1 at **a)** 30 µm, **b)** 1 µm, **c)** 300 nm

Dye degradation experiments and MnO_2-NP-WH catalyst reuse

For each degradation test, the variation of the dye concentration was monitored measuring the UV-Vis absorbance at λ = 600 nm, using a pre-established calibration curve. The amount of dye absorbed (q) at any time t was calculated from equation [2].

$$q_t = \frac{V(C_O \quad C_t)}{W} \qquad [2]$$

Where, at equilibrium *e*, $q_t = q_e$ and $C_t = C_e$. And C_o, C_t and C_e are the initial, any time, and equilibrium concentrations of the dye solutions (mg/L), respectively. *V* is the solution volume and *W* is the mass of adsorbent (*28*). The dye removal percentage [Re(%)] was calculated as follows:

$$\mathrm{Re}(\%)\ \frac{(C_0 - C_t)\cdot 100}{C_0} \qquad [3]$$

Prior to the degradation experiments, the catalyst was placed in a small sealed paper bag (similar to a tea bag) in order to prevent the MnO_2-NP-WH catalyst diffusion in the solution, facilitate the catalyst withdrawn process, and to slightly approach the experimental set up to an industrial design (Figure 4a).

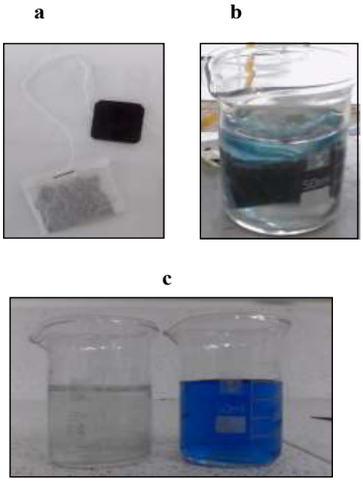

Figure 4. a) Paper bag with MnO_2-NP-WH inside **b)** Experimental set-up **c)** Color change of the solution before and after the contact with the MnO_2-NP-WH catalyst

The first degradation tests were conducted at pH 7 using 1.0 g of MnO_2-NP-WH catalyst in a 20 ppm solution of IC. No change in the initial dye concentration was observed during these attempts even after 2 h of contact. However, pH variations (2.3, 4.5 and 7.0) in additional experiments showed that the best results for IC removal were obtained at pH = 2.3 (Figure 4b-c). The IC removal efficiency comparison between the MnO_2-NP-WH catalyst synthesized (sample 1, 2 and 3) and the WH samples (Figure 5), showed that all nanobiocomposites had much better IC degradation rate than the non-modified WH, pretreated WH, and also to the activated carbon, evaluated as absorbent solid. It must be noted that MnO_2-NP-WH sample 2 is the fastest IC degradation catalyst, requiring only 5 min to achieve the 97.6% dye removal. For the same degradation results, the activated carbon needed more than 50 min.

This removal effectiveness at lower pH conditions is favored by the presence of $-SO_3^-$ groups over the IC structure (*27*). As a consequence, at acidic conditions, the MnO_2-NP-WH bionanocomposite surface is protonated, increasing the electrostatic interactions with the IC molecules as well as the degradation rate.

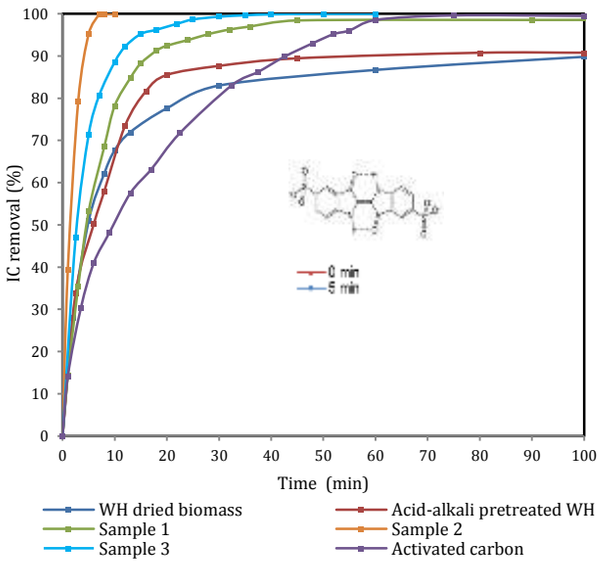

Figure 5. Dye removal at 22°C and pH = 2.3. Insert: UV-Vis monitoring of IC color removal

To support the above hypothesis, the pH_{pzc} of the biocomposite was determined. The point of zero charge (pzc) describes the condition when the electrical charge on a surface is zero and it is frequently determined in relation to an electrolyte's pH. In other words, pH_{pzc} is usually the pH value at which a solid submerged in an electrolyte exhibits zero net electrical charge on the surface (*29*). Therefore, in NP synthesis, cations adsorption is favored at pH > pH_{pzc}, while the anions adsorption is favored at pH < pH_{pzc} (*30*). For the WH biomass a value of pH_{pzc} = 4.5 was obtained, which means that WH surface is positive charged at pH < 4.5. Then, there is a strong electrostatic interaction between the WH surface and the IC molecules at low pHs, promoting the dye adsorption and degradation. Similarly, other studies reveal the high dependence of the MnO_2 surface on the pH solution, in those a pH_{pzc} value between 4-5 was determined as optimal (*20, 31*).

The temperature effect on IC degradation was tested for MnO_2-NP-WH sample 2 at pH = 2.3. The results show that the bionanocomposite performs better at low temperatures (Figure 6), which is a positive variable in the case of scaling up experiments. The physicochemical explanation and implications of these results are under studying at moment by this group.

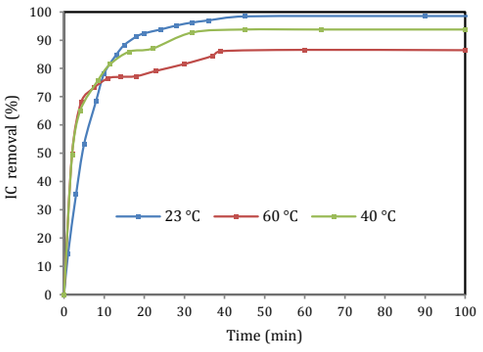

Figure 6. IC removal in time by varying temperature at pH ~ 2.3 for sample 2

To measure the reuse capacity of the MnO_2-NP-WH catalysts, sachets with 0.5 g of bionanocomposite were sequentially placed into seven different IC fresh prepared solutions; the characteristic absorption in each solution was followed by UV-Vis after 5 min contact (Figure 7). The results showed that the degradation capacity for the untreated WH was just 30% of the initial after seven cycles of usage. Meanwhile, by comparing the last cycle with the initial for MnO_2-NP-WH samples 1 and 3, the degradation capacity wass lightly reduced in just 5 and 3%, respectively. Interestingly, the dye removal of MnO_2-NP-WH sample 2 decreased abruptly after the sixth cycle of usage. The possible reasons for these variations in reuse capacity are: (i) occupation of available adsorption sites within the WH matrix by IC molecules and (ii) leaching of MnO_2 NPs to the solution, reducing the number of active reaction sites on the bionanocomposite surface.

In order to characterize the IC degradation products, the solution, before and after IC color removal process, was monitored by ESI-MS in negative ion mode. Similar to what was reported by Combariza *et al.* (*20*), the ESI-MS for the initial IC solution presented a unique and characteristic base peak at m/z 421, corresponding to IC in its anionic form (*32*). After 5 min of degradation, there was no signal for IC, instead, several peaks were shown at m/z 190, 226, 237, 253 and 257.9 (Figure 8). Among these signals, the peak at m/z 226 has been previously assigned to the oxidative breaking of the initial C=C bond and it have been identified as isatin sulfonic acid (*20, 32-34*).

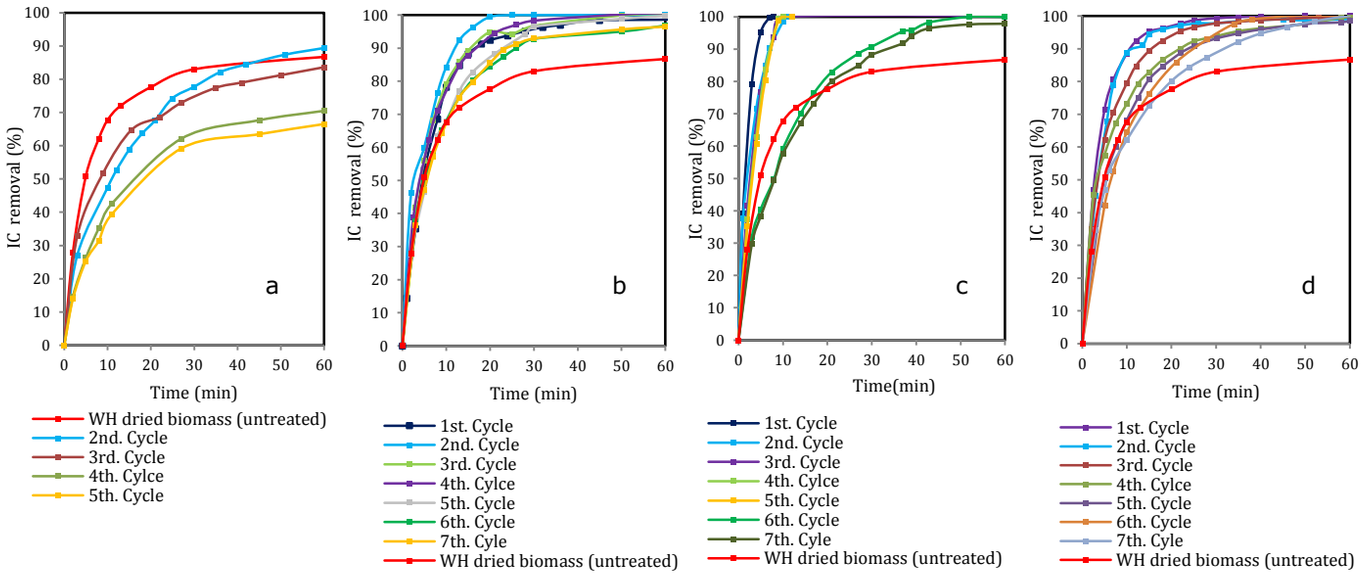

Figure 7. IC removal (T= 22°C, pH = 2.3) after consecutive reuse cycles. **a)** WH untreated; **b)** MnO_2-NP-WH sample 1; **c)** MnO_2-NP-WH sample 2; **d)** MnO_2-NP-WH sample 3

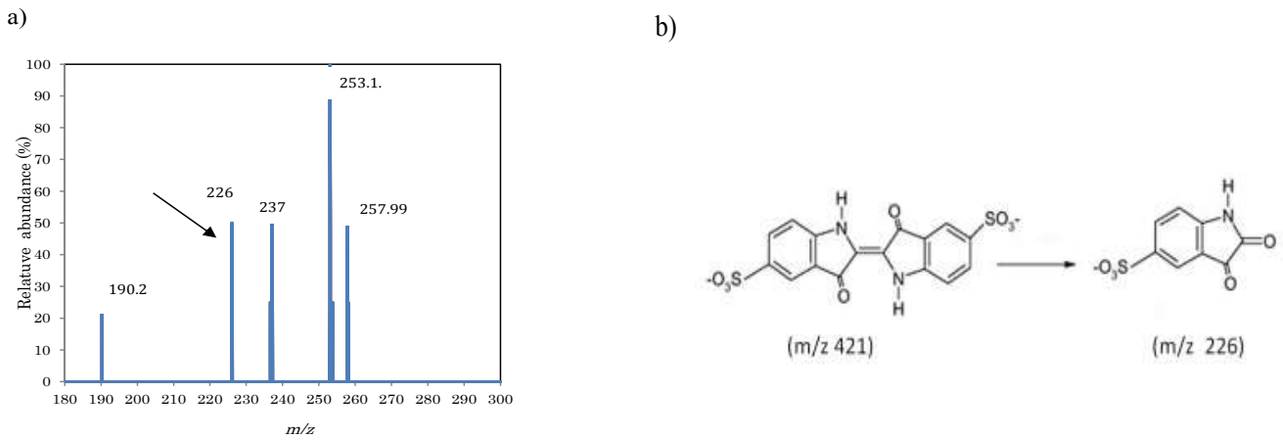

Figure 8. a) ESI-MS after a reaction time of 5 min; **b)** Indigo carmine (m/z 421) and isatin sulfonic acid (m/z 226), one of the few degradation products identified

Conclusions

The water hyacinth (*Eichhornia crassipes*) has a great potential as solid matrix for the deposition of MnO_2 NPs and as catalyst in the organic dyes degradation, due to its surface morphology and high adsorbent capacity. It is therefore an economic and practical alternative for the solution of two current environmental issues: (i) water contamination, due to the extensive withdrawal of toxic dyes such as IC, and (ii) the invasion of water reservoirs caused by the WH extremely fast proliferation and growth, which presents serious environmental, economic, and navigation challenges, among others.

The NPs synthetic methods studied in this investigation, ethanol and ultrasonic-assisted, both provided suitable conditions for the deposition of MnO_2 NPs over cellulosic matrices under the described experimental parameters. It was found that the ethanol-assisted synthesis produces the highest deposition of manganese onto the pretreated WH (33.3%) in comparison with the ultrasonic bath (28.7%) and horn-assisted (21.7%) synthesis. However, the leaching of MnO_2 particles is considerable lower after the ultrasonic synthesis and the catalyst reuse produces therefore better results by this synthetic methodology.

The results showed that the MnO_2-NP-WH bionanocomposites constitute effective catalysts for the IC degradation in aqueous solution at 23 °C, pH = 2.3 and 5 min contact time. Under these conditions, 97.6% of IC can be degraded (percentage as function of decrease in absorbance at the λ_{max} for IC). Finally, the mass spectrometry analysis evidenced that although some pure absorption processes by the WH matrix cannot be ruled out, a chemical degradation of the dye was confirmed.

References

1. Saha, S.; Pal, A. Microporous assembly of MnO_2 nanosheets for malachite green degradation. *Sep. and Purif. Technolgy*. **2014**, *134*, 26-36. DOI: http://dx.doi.org/10.1016/j.seppur.2014.07.021.
2. Priya, E. S.; Selvan, P. S. Water hyacinth (*Eichhornia crassipes*) – An efficient and economic adsorbent for textile effluent treatment-A review. *Arabian J. Chem.* **2014**. DOI: http://dx.doi.org/10.1016/j.arabjc.2014.03.002.
3. Vautier, M.; Guillard, C.; Herrmann, J. M. Photocatalytic Degradation of Dyes in Water: Case Study of Indigo and of Indigo Carmine. *J. Catal.* **2001**, *201* (1), 46-59. DOI: http://dx.doi.org/10.1006/jcat.2001.3232.
4. Palma, R. E; Macías, J.; González, I.; Torres, R. A. Tratamiento de aguas residuales provenientes de la industria textil mediante oxidación electroquímica. *Rev. Colomb. Mater*. **2013**, *4*, 93-108.
5. Barka, N.; Assabbane, A.; Nounah, A.; Ichou, Y. A. Photocatalytic degradation of indigo carmine in aqueous solution by TiO_2-coated non-woven fibres. *J. Hazard. Mater*. **2008**, *152* (3), 1054-1059. DOI: http://dx.doi.org/10.1016/j.jhazmat.2007.07.080.
6. Rauf, M. A.; Ashraf, S. S. Radiation induced degradation of dyes—An overview. *J. Hazard. Mater.* **2009**, *166* (1), 6-16. DOI: http://dx.doi.org/10.1016/j.jhazmat.2008.11.043.
7. Ahmed, K. A. M.; Peng, H.; Wu, K.; Huang, K. Hydrothermal preparation of nanostructured manganese oxides (MnOx) and their electrochemical and photocatalytic properties. *Chem. Eng. J. (Amsterdam, Neth.)* **2011**, *172* (1), 531-539. DOI: http://dx.doi.org/10.1016/j.cej.2011.05.070.
8. Yu, C.; Li, G.; Wei, L.; Fan, Q.; Shu, Q.; Yu, J. C. Fabrication, characterization of β-MnO_2 microrod catalysts and their performance in rapid degradation of dyes of high concentration. *Catal. Today* **2014**, *224* (0), 154-162. DOI: http://dx.doi.org/10.1016/j.cattod.2013.11.029.
9. Maliyekkal Shihabudheen, M.; Kinattukara Lisha, P.; Pradeep, T. A novel cellulose–manganese oxide hybrid material by in situ soft chemical synthesis and its application for the removal of Pb(II) from water. *J. Hazard. Mater*. **2010**, *181*, 986-995. DOI: http://dx.doi.org/10.1016/j.jhazmat.2010.05.112.
10. Zhang, W.; Yang, Z.; Wang, X.; Zhang, Y.; Wen, X.; Yang, S. Large-scale synthesis of β-MnO_2 nanorods and their rapid and efficient catalytic oxidation of methylene blue dye. *Catal. Commun*. **2006**, *7* (6), 408-412. DOI: http://dx.doi.org/10.1016/j.catcom.2005.12.008.
11. Sui, N.; Duan, Y.; Jiao, X.; Chen, D. Large-Scale Preparation and Catalytic Properties of One-Dimensional α/β-MnO_2 Nanostructures. *J. Phys. Chem C*. **2009**, *113* (20), 8560-8565. DOI: http://dx.doi.org/10.1021/jp810452k.
12. Invasive Species Compendium, Datasheet *Eichhornia crassipes*. https://www.invasivespeciesinfo.gov/aquatics/waterhyacinth.shtml (accessed November 1st 2015).
13. Téllez, T. R.; López, E. M. D. R.; Granado, G. L.; Pérez, E. A.; López, R. M.; Guzmán, J. M. S. The water hyacinth, *Eichhornia crassipes*: an invasive plant in the Guadiana River Basin (Spain). *Aquatic Invasions* **2008**, *3* (1), 42-53. DOI: http://dx.doi.org/10.3391/ai.2008.3.1.8.
14. Lin, S.; Wnag, G.; Na, Z.; Lu, D.; Liu, Z. Long-root *Eichhornia crassipes* as a biodegradable adsorbent for aqueous As (III) and As (V). *Chem. Eng. J.* **2012**, *183*, 365-371. DOI: http://dx.doi.org/10.1016/j.cej.2012.01.013.
15. Komy, Z. R.; Abdelraheem, W. H.; Ismail, N. Biosorption of Cu^{2+} by *Eichhornia crassipes*: Physicochemical characterization, biosorption modeling and mechanism. J. *King Saud. Univ. Sci.* **2013**, *25*, 47-56. DOI: http://dx.doi.org/10.1016/j.jksus.2012.04.002.
16. Zheng, J. C.; Feng, H. M.; Lam, M. H.W.; Lam, P. K.S. Removal of Cu(II) in aqueous media by biosorption using water hyacinth roots as a biosorbent material. *J. Hazard. Mater*. **2009**, *171*, 780-785. DOI: http://dx.doi.org/10.1016/j.jhazmat.2009.06.078.
17. National Environment Protection Council NEPC Schedule B3: Guideline on Laboratory Analysis of Potentially Contaminated Soils, 2011. http://goo.gl/g0uQz4 (accessed December 12 2015).
18. Wang, H..; Zheng, M.; Chen, J.; Ji, G.; Cao, J. M. Synthesis of MnO_2 Microfiber with Secondary Nanostructure by Cotton Template. *J. Nanotech.* **2010**, *2010*. DOI: http://dx.doi.org/10.1155/2010/479172.
19. Zhu, S.; Zhang, D.; Li, Z.; Furukawa, H.; Chen, Z. Precision Replication of Hierarchical Biological Structures by Metal Oxides Using a Sonochemical Method. *Langmuir* **2008**, *24*, 6292-6299. DOI: http://dx.doi.org/10.1021/la7037153.
20. Chacón Patiño, M. L.; Blanco Tirado, C.; Hinestroza, J. P.; Combariza, M. Y. Biocomposite of nanostructured MnO_2 and fique fibers for efficient dye degradation. *Green Chem*. **2013**, *15*, 2920–2928. DOI: http://dx.doi.org/10.1039/C3GC40911B.

21. Kumar, P.; Barrett, D. M.; Delwiche, M. J.; Stroeve, P. Methods for Pretreatment of Lignocellulosic Biomass for Efficient Hydrolysis and Biofuel Production University of California. *Division of Agriculture and Natural Resources* [Online], 2009. http://ucanr.edu/datastoreFiles/234-1388.pdf (accessed August 26th 2015).
22. Esteghlalian, A.; Hashimoto, A. G.; Fenske, J. J.; Penner, M. H. Modeling and optimization of the dilute-sulfuric-acid pretreatment of corn stover, poplar and switchgrass. *Bioresour. Tech.* **1997**, *59* (2–3), 129-136. DOI: http://dx.doi.org/10.1016/S0960-8524(97)81606-9.
23. Ganguly, A.; Das, S.; Bhattacharya, A.; Dey, A.; Chatterjee, P. K. Enzymatic hydrolysis of water hyacinth biomass for the production of ethanol. Optimization of giving parameters. *Indian J. Exp. Biol.* **2013**, *51*, 556-566.
24. Agbor, V. B.; Cicek, N.; Sparling, R. Biomass pretreatment: Fundamentals toward applicaton. *Biotechnol. Adv.* **2011**, *29*, 675-685. DOI: http://dx.doi.org/10.1016/j.biotechadv.2011.05.005.
25. Subramanian, V.; Zhu, H.; Wei, B. Alcohol-assisted room temperature synthesis of different nanostructured manganese oxides and their pseudocapacitance properties in neutral electrolyte. *Chem. Phys. Lett.* **2008**, *453*, 242-249. DOI: http://dx.doi.org/10.1016/j.cplett.2008.01.042.
26. Chacón, M.L. Síntesis *in situ* y caracterización de nanopartículas de óxidos de manganeso en fibras de fique y su aplicación en el tratamiento de agua contaminada con colorantes. MSc. Thesis, UIS, Bucaramanga, 2011.
27. Al-Degs, Y. S.; El-Barghouthi, M. I.; El-Sheikh, A. H.; Walker, G. M. Effect of solution pH, ionic strength, and temperature on adsorption behavior of reactive dyes on activated carbon. *Dyes Pigm.* **2008**, *77* (1), 16-23. DOI: http://dx.doi.org/10.1016/j.dyepig.2007.03.001.
28. Elmorsi, T., Equilibrium Isotherms and Kinetic Studies of Removal of Methylene Blue Dye by Adsorption onto Miswak Leaves as a Natural Adsorbent. *J. Environ. Protection* **2011**, *2*, 817-827.
29. Singha, S.; Sarkar, U.; Mondal, S.; Saha, S. Transient behavior of a packed column of Eichhornia crassipes stem for the removal of hexavalent chromium. *Desalination* **2012**, *297* (0), 48-58. DOI: http://dx.doi.org/10.1016/j.desal.2012.04.016.
30. Lakshmi, U. R.; Srivastava, V. C.; Mall, I. D.; Lataye, D. H. Rice husk ash as an effective adsorbent: Evaluation of adsorptive characteristics for Indigo Carmine dye. *J. Environ. Manage.* **2009**, *90* (2), 710-720. DOI: http://dx.doi.org/10.1016/j.jenvman.2008.01.002.
31. Grządka, E. The Adsorption Layer in the System: Carboxymethylcellulose/Surfactants/NaCl/MnO2. *J. Surfact. Deterg.* **2012**, *15* (4), 513-521. DOI: http://dx.doi.org/10.1007%2Fs11743-012-1340-5.
32. Dalmázio, I.; de Urzedo, A. P.; Alves, T.; Catharino, R. R.; Eberlin, M. N.; Nascentes, C. C. *et al.* Electrospray ionization mass spectrometry monitoring of indigo carmine degradation by advanced oxidative processes. *J. mass spectrom.* **2007**, *42* (10), 1273-1278. DOI: http://dx.doi.org/10.1002/jms.1159.
33. Coelho M.G. ; Lima G.M.; Augusti, R.; Maria, D.A.; Ardisson, J.D. New materials for photocatalytic degradation of Indigo Carmine—Synthesis, characterization and catalytic experiments of nanometric tin dioxide-based composites. *Appl. Catal. B: Environ.* **2010**, *96*, 67-71. DOI: http://dx.doi.org/10.1016/j.apcatb.2010.02.002.
34. Zaied, M.; Peulon, S.; Bellakhal, N.; Desmazieres, B.; Chaussé, A. Studies of N-demethylation oxidative and degradation of methylene blue by thin layers of birnessite electrodeposited onto SnO_2. *Appl. Catal. B: Environ.* **2011**, *101* (3), 441-450. DOI: http://dx.doi.org/10.1016/j.apcatb.2010.10.014.

Article citation:
Cuervo-Blanco, T.; Sierra, C. A.; Zea, H. R. Nanostructured MnO_2 catalyst in *E. crassipes* (water hyacinth) for indigo carmine degradation. *Rev. Colomb. Quim.* **2016**, *45* (2), 30-38. DOI: http://dx.doi.org/10.15446/rev.colomb.quim.v45n2.60395.